Evaluating the Profile Geochemical Characteristics and Environmental Risk Prediction of Typical Sulfide Tailing Ponds Through Multiple Methods

Liqun Zhang
Anhui University
Xing Chen
Anhui University
Chunlu Jiang
Anhui University
Liugen Zheng (lgzheng@ustc.edu.cn)
Auhui University
Yiming Xia
Anhui University
Zheng Qiu
Anhui University

Research Article

Keywords: Tailings, Geophysics, Geochemistry, Mineralogy, Risk assessment

Posted Date: June 24th, 2021

DOI: https://doi.org/10.21203/rs.3.rs-578596/v1

Abstract

Abandoned tailings generated from copper mining are exposed to the environment for a long time will cause related risks, such as stability, landslides, surface and groundwater pollution, acid mine drainage (AMD) and secondary mineral deposits. This research started from multiple methods and comprehensively assessed the current status of mine tailings through the joint application of geophysics, geochemistry and mineralogy techniques to identify relevant environmental hazards. A thick oxidized hardened layer was formed on the surface of the tailings dam, but there were still faults or crack that affected its structural stability. According to the low-resistivity distribution of the tailings, the surface oxide compaction was judged, and the existence of high-resistivity cracks judged the potential migration path of heavy metals (HMs). The microscopic morphology and existing mineral phases of tailings particles at different depths in the profile were determined by SEM and XRD of representative samples as the main feature of iron crystalline phase. As the profile depth increased, the minerals such as calcite, pyrite and goethite gradually appeared. In addition, Cr and As were no risk, Cu, Zn, Pb were low risk, Ni was medium risk, and Cd was high risk in risk assessment code (RAC) analysis of the tailings. Judging whether HMs in the tailings are hazardous substances according to the results of toxicity characteristic leaching procedure (TCLP), it was found that the leaching contents of Cu, Zn, Pb, Cr, Ni, As were all lower than the limit, while the leaching content of Cd was higher than the limit, and additional attention should be paid to Cd pollution.

1 Introduction

The mining of iron ore requires the construction of dams in order to dispose of the waste after treatment. The waste produced in the process of extracting valuable elements from the ore is called tailings (Orlando et al., 2020). Usually mine tailings sediments are not suitable for plant growth due to low carbon and nitrogen content, high acidity, salt conditions and heavy metal content. In addition, these tailings sediments also bring related environmental hazards such as landslides caused by geotechnical instability, dam damage, infrastructure damage or sandstorms, and potentially toxic metals immersed in groundwater (Conesa et al., 2006; Zheng et al., 2019a; Zanuzzi et al., 2009; Chen et al., 2020). Among them, the oxidation of sulfide ultimately produces a highly acidic leaching solution of high concentration of sulfate, iron and other heavy metals, which is called acid mine drainage. Therefore, in order to ensure the long-term environmental integrity of the tailings pond, it is important that the sulfide minerals contained are not quickly decompose and promote the leaching of heavy metals (Martínez-Pagána et al., 2011). Sulfide deposits contain large amounts of copper, nickel, zinc, lead and other economically important metals, usually in chalcopyrite ($CuFeS_2$), sphalerite ((Zn, Fe) S) and galena (PbS), and gangue minerals such as pyrite and pyrrhotite are the dominant sulfide combinations (Lindsay et al., 2015). In addition, the soil near the mining area shows high concentrations of inorganic pollutants, which come from mine tailings ponds or smelters, and are present in sedimentary (metal colloidal) particles of complex mineral composition (Tuhý et al., 2020). Therefore, if you want to understand the degree of sulfide oxidation and whether there are potential buffer minerals and secondary mineral deposits,

detailed mineralogy of tailings is required (Heikkinen and Räisänen., 2008). This is the basis for understanding and solving the environmental pollution problem of tailings ponds, and is the first step to prevent harmful metal elements from entering the surrounding ecological environment, and to effectively manage and repair tailings ponds.

For abandoned tailings ponds, the restoration process is an important step in reducing environmental and human health risks. Therefore, evaluating the composition of this waste will contribute to make disposal decisions. At present, many scholars are engaged in mining-related research by using different geophysical technologies. Electrical resistivity tomography (ERT) has been widely used for near-surface exploration in landslide areas characterized by complex geological environment, such as understanding the relationship between resistivity value and geotechnical properties, judging whether the geological characteristics of tailings dams are suitable for accumulation of tailings, and the acid production capacity (Gómez-Ortiz et al., 2010; Zarroca et al., 2015; Kuranchie et al., 2015; Khoeurn et al., 2019). However, using only one hole per meter in the ERT requires huge economic costs and is not the best method to reveal the characteristics of tailings pond. Therefore, combining geochemical techniques, mineralogical characteristics, and a reasonable number of ERTs can provide a powerful and reliable characterization of the entire site. In addition, most previous studies of tailings geochemistry and mineralogy (DeSisto et al., 2011; Liu et al., 2018; Chappell and Craw., 2002) have focused on the strongly weathered surface layer, which is relatively narrow and generally and not extend more than a meter deep. However, generally the characteristics of mineral distribution and heavy metal content are quite different between the surface layer and the lower layer of tailings. Therefore, it is necessary to compare and analyze the chemical composition difference between the surface layer and the lower layer of tailing pond, so as to fully identify the characteristics of tailing pond.

In this research, we proposed the ERT method based on the network parallel electrical method as a geophysical technology. In order to better determined the actual condition of the tailings pond and solved its environmental integration problem in a harmless manner, it is necessary to combine the geophysics, geochemistry and mineralogical knowledge to analyze the profile geological and environmental characteristics of the tailings pond. The key functions of this study were as follows: (1) determined the stability of the tailings pond and highlight the faults or fracture areas in the profile that may affect the structural stability. (2) discussed the influence of element enrichment and migration on the oxidation degree of tailings. (3) Screened out the environmental concerns needed by tailings pond and evaluated its environmental risks. On this basis, a comprehensive evaluation of the pollution status of the tailing pond can provide theoretical support for surrounding soil remediation. The results of the study can help other staff to mark the priority route for heavy metal transportation or acid mine drainage, which is very important for better mine soil remediation.

2 Methodology

2.1 Site description

The study area (30°45'-31°09'N, 117°35'-118°09'E) is located in southern Anhui Province, China (Fig. 1). The tailings pond was at the edge of the mining area, surrounded by mountains on three sides, and there had a primary stone-built dam underneath the dam. The valley-type tailings pond, mainly comes from the flotation and sweeping process of the concentrator, was abandoned in 2004 and planned to be repaired (Zheng et al., 2019b). The tailings pond is located in the middle section of the middle and lower reaches of the Yangtze River metallogenic belt on the northern margin of the Yangtze Craton. The area has experienced three periods of tectonic movement, namely the neoproterozoic nanhua period to early, middle and late triassic and sedimentary caprock formed after Cenozoic collision orogeny (Xu et al., 2013; Yang et al., 2014). The outcrop stratigraphic sequence of the mining area is dominated by the Silurian to Cretaceous sedimentary units, the Upper Carboniferous-Lower Permian Huanglong Formation, Chuanshan Formation, Middle Permian Qixia Formation, Upper Permian Dalong Formation, and Lower Triassic The Yinkeng Formation, Longshan Formation and Nanlinghu Formation are ore-bearing horizons (Tang et al., 2013; Zhang et al., 2020). Since the Mesozoic, the middle and lower reaches of the Yangtze River, including the study area, have entered a period of active tectonic movement. The strong tectonic movement in the Yanshan period led to the activity of intermediate-acid magma, and the extensive exposure of intermediate-acid magma led to the mineralization of heavy metals such as copper, zinc, and gold (Liu et al., 2020; Cao et al., 2017). The study area has a subtropical humid monsoon climate and belongs to a zone with variable climate and large annual changes in precipitation. The summer is very hot and rainy, and the winter is short. Rainfall drainage can easily cause tailings to be washed downstream, and there are more residential areas under the tailings dam (Shen et al., 2019).

2.2 Sampling

Selected a typical profile with both an oxidized layer and an unoxidized layer in the tailings pond. According to the color of the section, knocked out the block samples of surface hardened layer, and used the groove method to continuously sample scientifically (Huang et al., 2014). The green-gray tailings at the profile bottom can be taken with a spade shovel directly. This sampling used 0.5 m spacing to reduce the impact of uneven tailings particle size on the analysis results. From the hardened layer in top to the loose layer which is close to the original color of the tailings, a total of 11 tailings samples were collected (Fig. 1). Put it into a sealed bag and indicate the sample number to ensure that the sample is not contaminated. All the samples collected were air-dried naturally, and then crushed in an agate mortar to pass through a 100-mesh sieve for different experiments.

2.3 Analytical methods

2.3.1 Electrical resistivity tomography

Electrical resistivity tomography (ERT) is a physical technology that continuously measures the potential duration curves of all measuring electrodes while supplying power, and obtains the response potential of any electrode's natural field, primary field, and secondary field by uncompiling the space-time curves of current and potential obtained by excitation (Bai et al., 2016). And combined with RES2DINV for inversion processing to obtain the resistivity profile of the tailings accumulation. In this study, a total of 32

electrodes were arranged on the tailings accumulation dam in a linear observation mode with a spacing of 2m and a total detection length of 62 m. In order to prevent the infinite B pole from interfering with the data collection, the B pole was placed far away. The actual data collection was carried out by the ABM method, which is any two electrodes form a dipole power supply (AB pole), and the remaining 30 electrodes (M pole) collect potential data at the same time. The acquisition parameters were 0.5s constant current, 50ms sampling interval, single positive acquisition current, and about 0.5 h single acquisition time.

2.3.2 Geochemical analysis

Tailings were compressed under a pressure of 40 t for 60 s, and pressed it into a disc with a sample diameter of 32mm and a border outer diameter of 40mm with a boric acid film at the bottom, and then the major elements were determined by XRF (MXPAHF, Rigaku Industrial Corporation, Japan).

The 10 ml of 10% H_2O_2 was added into tailings and boiled to made it fully reacted, then added 10 ml of 10% HCl to boil and fully react. The beaker was filled with distilled water for 24 hours, distilled water was removed, 10 ml of dispersant $(NaPO_3)_6$ with a concentration of 0.05 M was added, and the ultrasonic cleaner was shaken for 7 minutes and then the particle-size of tailings profile were determined by laser particle size analyzer (LS13320, Beckman Coulter, USA). The test range of the analyzer was 0.02 ~ 2000μm, and repeated measurement error is less than 2%.

The total amount of HMs was digested with an electric heating plate by the mixed acid digestion method. At the same time, three sets of parallel samples were required to take the average value to ensure the accuracy of the test. The chemical fraction distribution of HMs was determined through the BCR extraction method (Rodríguez et al., 2009), and the extraction rate was 90–110%. The experimental procedure of TCLP and the selection of extraction fluid have been published in the previous report (Zhang et al., 2021). The samples obtained in this step were all determined by ICP-AES (7400, Thermo Fisher Scientific Inc, USA).

2.3.3 Microstructure and mineralogy

Evenly selected the surface and bottom samples, fixed them with silver glue and sprayed gold film, and micromorphology was observed by SEM (S-4800, Hitachi Corporation, Japan). The working parameters of the SEM were 1.4 nm secondary electron resolution, 15 kV acceleration voltage, about 5 mm working distance, and about 50 ns SEM image retention time. Another sample was taken for boiling treatment and prepared as a 30 mm thick polished sheet for observation of mineralogy under optical microscope (BX53, Olympus, Japan). The microscope condition was manual focusing, the lifting range was 50mm, and the visual magnification was 40X-500X. The mineral crystals in the tailings were irradiated by XRD (SmartLab9, Rigaku Industrial Corporation, Japan) within the range of $10° < 2\theta < 70°$, each step counting time was 0.5 s, and combined with MDI Jade and Origin 2018 to qualitative analysis the spectrum peaks, identified the mineral components contained in the tailings. The above experiments were completed in the laboratory of the modern experimental technology center of Anhui University.

3 Results And Discussion

3.1 Basic indicators

The pH range was between 3.62 and 7.78, with an average of 5.09, and showed an increasing trend with the increase of profile depth. The acidic surface tailings were mainly caused by the oxidation of metal sulfides to produce an acidic environment. As the depth increases, the oxidation environment weakens, and the pH gradually rises and stabilizes. The content of MC was low, with an average of 0.56, and there was no obvious change with the increase of profile depth (Table 1).

Table 1
Basic indicators of tailings

Profile depth/ m	0	-0.5	-1	-1.5	-2	-2.5	-3	-3.5	-4	-4.5	-5
pH	3.62	3.66	3.67	3.87	3.75	4.25	4.89	5.34	6.19	7.66	7.78
MC	0.42	0.43	0.55	0.52	0.56	0.61	0.59	0.62	0.61	0.58	0.64
Note: “MC”-moisture content/ %											

3.2 Particle size distribution

Tailings in different layers have different particle size distribution characteristics. The larger the particle size distribution is, the higher the particle content is in the tailings. Meanwhile, the degree of oxidation of metal sulfide is not only related to oxygen and water, but also has a great influence on the particle size distribution of tailings (Jakubek et al., 2018; Silveira et al., 2018; Kang et al., 2018). In this study, the particle-size classification was: coarse sand (1 ~ 0.5 mm), medium sand (0.5 ~ 0.25 mm), fine sand (0.25 ~ 0.125 mm), very fine sand (0.125 ~ 0.063 mm), silt sand (0.063 ~ 0.002 mm) and clay (< 0.002 mm) (Fan et al., 2021). As shown in Fig. 2, the particle size of tailings was mainly distributed in 0.002 ~ 0.5 mm, and the particle size distribution changed greatly with the depth of tailings. The particle size of tailings at 0m ~ 1m was mainly distributed between 100 μm and 1000 μm, of which coarse sand, medium sand and fine sand were mostly. The particle size of the tailings at 1m ~ 5m was mainly distributed between 10 μm and 100 μm, of which fine sand, very fine sand and silt were mostly. Larger particles make it easy for rain and air to react with minerals on the surface and make the surface harder.

3.3 Resistivity of tailings accumulation

Electrical resistivity tomography (ERT) is a physical technology. The RES2DINV two-dimensional inversion program is an inversion calculation program based on the smooth constrained least squares method. It can use the new optimization nonlinear least squares algorithm to greatly improve the resolution of the direct current method and better reflect the underground apparent resistivity (Hsu et al., 2010; Theoharatos., 2008). Figure 3 was the resistivity profile of accumulated tailings obtained by two linear survey lines. The detection depth of the parallel electrical method was about 12m, and the average resistivity of tailings was about 400Ω·m, and the average resistivity of tailings was generally low due to

low water content. However, there was an obvious low-resistance anomaly area of about 1.2 m in the surface layer because the HMs on the surface of the tailings have been leached by rainwater for a long time, and the accumulation time was longer, which caused the continuous penetration of water and air, causing the tailings to continue to oxidize and form a hardened layer of oxidation. The formed hardened layer can limit the continuous infiltration of acid leachate and the oxidation of sulfide, reducing the oxidation rate of tailings (Ahn et al., 2011). In addition, the surface has a larger particle size (Fig. 2), high water permeability, and a high content of conductive minerals (sulfide) (Fig. 4). As the increase of depth profile, the particle size shows a decreasing trend, and the S content gradually decreases and then stabilizes. This is the reason why the resistivity of surface is low and bottom is high (Fig. 3). In the profile with decreasing granularity, fine metal sulfide minerals are not suitable for flotation, so fine materials can retain most of the water, and the vertical flow gradually slowed down and prevented the formation of large areas in strong oxidation zone (Nikonow et al., 2019). But in the process of moving to south resistivity changed, 30 m in horizontal direction at high resistance was unusual, this was because the artificial mining activities led to the consolidation or less tailings stacking the uneven and produce cracks, increased resistivity. Hazardous transmission of acid mine waste water (AMD) or HMs pollutants was present here, reflecting that may affect the structural stability of faults, or cracks (Fig. 3a). At the edge of the profile, the resistance was higher due to the weathering of the tailings, the evaporation of water and the lower ion concentration (Fig. 3b).

3.4 Distribution characteristics of major and trace elements

As shown in Fig. 4, and the relevant data was shown in Table S1. The sequence of sulfide minerals was $Fe_2O_3 > SiO_2 > CaO > Al_2O_3 > MgO > K_2O > Na_2O$. The contents of Fe, Si and Al were 47.11%, 29.04% and 3.11%, respectively, which was consistent with the results of XRD analysis (Fig. 6), indicating that the composition of iron ore was mainly composed of pyrite, magnetite, pyrrhotite, goethite and other iron oxide and quartz, and consists of a small part of aluminum silicate. The average content of Fe_2O_3 in hardened layer was 41.41%, and that in weak oxide layer and loose layer was 32.05%, and the content decreased with the increase of depth. The average content of S reached 4.97%, which was mainly concentrated in hardened layer and tends to be stable with the profile depth, and was the main element for producing acidic wastewater. The contents of SiO_2 and CaO at different depths in the profile was stable, and the average content respectively was 24.24% and 17.4%. Tailings containing a lot of SiO_2 and CaO could be used as brick materials (Kim et al., 2019), which could not only make full use of mineral resources, but also be an important means to protect the ecological environment. The content of MgO in hardened layer was lower than that in loose layer, which was mainly related to the leaching degree of surface runoff, while the content of other compounds did not change much with the increase of profile depth.

The elements in Table S2 were included in the list of priority pollutants of USEPA. It showed that the relative abundance of the average HMs contents in tailings profile followed the sequence: Cu > Zn > Hg > As > Pb > Cr > Ni > Cd, and the average contents of Cu, Cd, Zn and As respectively were 1865.30 mg/kg, 1.39 mg/kg, 774.39 mg/kg and 78.34 mg/kg, reaching 37.31 times, 4.63 times, 3.87 times and 1.96 times

of the risk screening value in GB15618-2018. The average contents of Pb was 68.84 mg/kg and Ni was 42.95 mg/kg, which was lower than the risk screening value. It can be seen from Fig. 5 that the content of Hg and As in hardened layer was higher than that in loose layer, exposure of sulfide to air and water would cause the acidic leaching solution to release high concentrations of Hg and As that were easily adsorbed and precipitated by iron hydroxide, and are then enriched in oxidized hardened layer. The content of Cd in the hardened layer (0.66 mg/kg) was significantly lower than that in the non-oxidized layer (1.81 mg/kg), the main reason was that Cd was a sulfide associated element, and the oxidation process led to the consumption of Cd, Co and other sulfide associated elements in the tailing (Alakangas et al., 2006). The contents of Cu, Zn, Cr and Ni in the hardened layer were lower than that in the loose layer. This was because the HMs migrate to the surrounding area through rainwater leaching, which led to pollute groundwater, surface water and river water, and thus affected the health of the residents below the dam through the aquatic food chain.

HMs pollutants associated with primary sulfur in tailings, and the oxidation of tailings can be released to the surroundings of trace metals, and the S accelerated leaching of HMs and the acidic waste water produced in the surface layer and local enrichment. In addition, the formation of secondary minerals affected the migration and transformation of HMs, its surface tended to adsorption of HMs, which aggravated the pollution of surrounding soil and water (Rodríguez et al., 2009; Hamberg et al., 2016). Meanwhile, the particle-size of tailings affected the migration of HMs, and the larger surface particle size led to less dust generated under the action of wind. Therefore, the pollution of the tailings to the surrounding environment was mainly the acidic mine waste water generated by rainwater scouring and the migration of HMs.

3.5 Mineralogical analysis of representative tailing samples

The color of the tailings hardened layer was brownish yellow, and the loose layer was gray-green. The mineralogy of tailings profile was evaluated by SEM, polarized light microscope and XRD. As shown in Fig. 6, the tailings in the hardened layer had a large particle-size, and the mineral phase was observed to be covered by a large number of tailings particles of different shapes and secondary minerals, and the rounded edges of the debris showed signs of physical or chemical wear (Fig. 6a). The main primary minerals were gypsum and quartz, the secondary minerals were jarosite, which produces alteration along the grain margin, and Muscovite (aluminium silicate) (Fig. 6b, c). The formation of gypsum minerals was attributed to the oxidation of sulfide minerals, and which released sulfate ions (Cihangir et al., 2018). Meanwhile, the external oxidation conditions affect the mineral composition and form of tailings. The important indexes of the oxidation process of tailings were goethite and hematite, and jarosite sediments can be formed through mineral dissolution and reprecipitation to promote the formation of oxidizing crusts (Tang et al., 2018; Redwan et al., 2012; Regelink et al., 2014). Jarosite was the main reason that causes the surface layer of tailings to be brownish yellow, and its content decreases with the decrease of oxidation degree. Mineral crystals in the loose layer were relatively complete and grow in layers (Fig. 6d). The primary minerals were gypsum, quartz, pyrite and feldspar. In addition to jarosite and muscovite, the secondary minerals also include pyrrhotite, goethite, sphalerite, and no obvious corrosion was observed

on the surface of mineral particles (Fig. 6e, f). The presence of Al, K and Na in tailings was attributed to muscovite, jarosite and feldspar, and the diffraction peak parameters were shown in Table S3. The metal sulfide mainly contains iron ore, which was related to the processing technology of concentrator (Zheng et al., 2019b).

The existence of metal colloid is limited by the mineralogy and geochemical composition of the tailings solid, but the fluidity in the pore water of tailings is controlled by the secondary sedimentation-dissolution and adsorption-desorption reactions as well as the biogeochemical redox process (Nordstrom., 2011). For example, Fe, Al, Zn and Cu will show higher dissolution concentration and greater mobility in acidic environment, while As, Se, Mo, Sb and other elements forming (hydrogen) oxygen anions can move in alkaline pore water (Majzlan et al., 2014). Calcite, pyrite and goethite and other mineral characteristics peak were not seen in hardened layer, but the peak gradually appeared with the increase of depth. It also indicated that surface silicate minerals showed strong characteristic peaks, while carbonate minerals and metal sulfide minerals appeared weak or even zero characteristic peaks, reflecting opposite characteristics with the increase of profile depth. This was because there is more free oxygen and free water on the surface, S and Fe mainly enriched in the surface layer, metal sulfide oxidation produce acid to dissolve primary metal minerals in acidic conditions to generate high acidity of pore water, is characterized by a high concentration of dissolved Fe. Carbonate minerals such as calcite react with acid to be consumed, resulting in less metal sulfide and carbonate minerals in the surface tailings. As the depth increases, the oxidation weakens and the characteristic peak becomes stronger. Subsequent dissolution of aluminosilicate minerals in the sulfide oxidation zone also contributed to the dissolution of Al, and acidic pore water migrated downward and was neutralized by dissolution of carbonate minerals (Moncur et al., 2005).

3.6 Chemical fraction and risk assessment

The environmental risk of tailings was predicted by using BCR sequential extraction and TCLP. The chemical fraction distribution of HMs in representative composite tailings was showed in Fig. 7a, Tables S4 and Table S5, and the different fractions of HMs were distributed as: Ni and Cr were F4 > F2 > F1 > F3, Cd was F4 > F1 > F2 > F3, Pb and Zn were F4 > F2 > F3 > F1, Cu was F4 > F3 > F1 > F2. From the perspective of fraction transformation behavior, most of HMs are in the residual (F4), especially arsenic. This fraction (F4) is considered unusable and not easy to release. The mobility of HMs is closely related to the content of bioavailable states. Therefore, the RAC index is established on the basis of the bioavailable state, and the ratio of bioavailable content to total content is divided into five levels to judge its risk level (Fig. 7b). Usually the first fraction (F1) has the greatest instability and environmental fluidity in the environment (Singh et al., 2005). According to RAC, Cr and As in tailings are no risk, Cu, Zn, and Pb are low risk, Ni is medium risk, and Cd is high risk. Pb and Cd with certain risks may limit the resource utilization of tailings. The identification standard values of hazardous waste under the supervision level of China and USEPA are listed in Table S6 (Zhang et al., 2021; Zhou et al., 2021). According to the TCLP results (Fig. 7b), the leaching content of Cu, Zn, Pb, Cr, Ni, As is below the limit, while the leaching content of Cd is higher than the limit, which is a hazardous material. Therefore, except for Cd, the tailings are relatively safe for

humans and the environment. However, there is still a risk of HMs pollution to the surrounding environment, and additional attention should be paid to Cd pollution.

4 Conclusion

Tailings contain a large number of valuable elements that can be used for secondary mining. The combination of geophysics, mineralography and geochemistry provides the geological and environmental characteristics of abandoned mines. The surface layer of tailings dam is formed with thick oxidized hardened layer, and the tailings dam is located at the southeastern edge of the tailings, the other three sides are surrounded by mountains, plus the primary dam of stone masonry under the tailings dam, resulting in a relatively stable tailings accumulation environment, but there are still faults or cracks affecting its structural stability. Calcite, pyrite and goethite and other mineral characteristics peak were not seen in hardened layer, but the peak gradually appeared with the increase of depth. Except for Cd, the toxicity leaching content of other HMs did not exceed the limit. The authorities should monitor HMs in the soil surrounding the tailings ponds, and concern for the environment is focused on the potential landslide and consequent release of highly polluting metals.

Declarations

Author contribution

Liqun Zhang: Methodology, Investigation, Software, Writing - original draft, Writing - review & editing. **Xing Chen, Chunlu Jiang:** Writing - review & editing. **Liugen Zheng:** Conceptualization, Resources, Funding acquisition, Supervision. **Yiming Xia:** Methodology, Data curation. **Zheng Qiu:** Data curation.

Funding

This work was supported by the National Natural Science Foundation of China (No. 42072201), and the Natural Science Foundation of Anhui Province (No. 1608085QD79).

Date availability

Not applicable

Ethical approval and consent to participate: Not applicable

Consent to publish: Not applicable

Competing interests: The authors declare that they have no known competing financial interests or personal relationships that could have appeared to influence the work reported in this paper.

References

1. Ahn JS, Song H, Yim GJ, Ji SW, Kim JG (2011) An engineered cover system for mine tailings using a hardpan layer: A solidification/stabilization method for layer and field performance evaluation. J Hazard Mater 197:153–160. https://doi.org/10.1016/j.jhazmat.2011.09.069
2. Alakangas L, Ohlander B (2006) Formation and composition of cemented layers in low-sulphide mine tailings, Laver, northern Sweden. Environ Geol 50(6):809–819. 10.1007/s00254-006-0253-x
3. Bai Z, Tan MJ, Zhang FL (2016) Three-dimensional forward modeling and inversion of borehole-to-surface electrical imaging with different power sources. Appl Geochem 13(3):437–448. 10.1007/s11770-016-0575-8
4. Chen X, Zheng L, Dong X, Jiang C, Wei X (2020) Sources and mixing of sulfate contamination in the water environment of a typical coal mining city, China: evidence from stable isotope characteristics. Environ Geochem Hlth 42(9):2865–2879. 10.1007/s10653-020-00525-2
5. Cihangir F, Ercikdi B, Kesimal A, Ocak S, Akyol Y (2018) Effect of sodium-silicate activated slag at different silicate modulus on the strength and microstructural properties of full and coarse sulphidic tailings paste backfill. Constr Build Mater 185:555–566. https://doi.org/10.1016/j.conbuildmat.2018.07.105
6. Conesa HM, Faz A, Arnaldos R (2006) Heavy metal accumulation and tolerance in plants from mine tailings of the semiarid Cartagena–La Union mining district (SE Spain). Sci Total Environ 366:1–11. https://doi.org/10.1016/j.scitotenv.2005.12.008
7. Chappell D, Craw D (2002) Geological analogue for circumneutral pH mine tailings: implications for long-term storage, Macraes Mine, Otago, New Zealand. Appl Geochem 17(8):1105–1114. https://doi.org/10.1016/S0883-2927(02)00002-1
8. Cao Y, Zheng Z, Du Y, Gao F, Qin X, Yang H, Lu Y, Du Y (2017) Ore geology and fluid inclusions of the Hucunnan deposit, Tongling, Eastern China: Implications for the separation of copper and molybdenum in skarn deposits. Ore Geol Rev 81(2):925–939. https://doi.org/10.1016/j.oregeorev.2016.04.013
9. DeSisto SL, Jamieson HE, Parsons MB (2011) Influence of hardpan layers on arsenic mobility in historical gold mine tailings. Appl Geochem 26(12):2004–2018. https://doi.org/10.1016/j.apgeochem.2011.06.030
10. Fan X, Xue Q, Liu S, Tang J, Qiao J, Huang Y, Sun J, Liu N (2021) The influence of soil particle size distribution and clay minerals on ammonium nitrogen in weathered crust elution-deposited rare earth tailing. Ecotox Environ Safe 208:111663. https://doi.org/10.1016/j.ecoenv.2020.111663
11. Gómez-Ortiz D, Martín-Velázquez S, Martín-Crespo T, Ignacio-San José C, Lillo J (2010) Application of electrical resistivity tomography to the environmental characterization of abandoned massive sulphide mine ponds (Iberian Pyrite Belt, SW Spain). Near Surf Geophys 8:65–74. https://doi.org/10.3997/1873-0604.2009052
12. Heikkinen PM, Räisänen ML (2008) Mineralogical and geochemical alteration of Hitura sulphide mine tailings with emphasis on nickel mobility and retention. J Geochem Explor 97(1):1–20. https://doi.org/10.1016/j.gexplo.2007.09.001

13. Huang J, Sheng XF, Xi J, He LY, Huang Z, Wang Q, Zhang ZD (2014) Depth-related changes in community structure of culturable mineral weathering bacteria and in weathering patterns caused by them along two contrasting soil profiles. Appl Environ Microbiol 80(1):29–42. 10.1128/AEM.02335-13
14. Hsu HL, Yanites BJ, Chen CC, Chen YG (2010) Bedrock detection using 2D electrical resistivity imaging along the Peikang River, central Taiwan. Geomorphology 114(3):406–414. https://doi.org/10.1016/j.geomorph.2009.08.004
15. Hamberg R, Bark G, Maurice C, Alakangas L (2016) Release of arsenic from cyanidation tailings. Miner Eng 93:57–64. https://doi.org/10.1016/j.mineng.2016.04.013
16. Jakubek ZJ, Chen MH, Couillard M, Leng TY, Liu L, Zou S (2018) Characterization challenges for a cellulose nanocrystal reference material: dispersion and particle size distributions. J Nanopart Res 20(4) 10.1007/s11051-018-4194-6
17. Khoeurn K, Sasaki A, Tomiyama S, Igarashi T (2019) Distribution of Zinc, Copper, and Iron in the Tailings Dam of an Abandoned Mine in Shimokawa, Hokkaido, Japan. Mine Water Environ 38(1):119–129. 10.1007/s10230-018-0566-5
18. Kuranchie F, Shukla S, Habibi D (2015) Electrical resistivity of iron ore mine tailings produced in Western Australia. Int J Min Reclam Env 29(3):191–200. 10.1080/17480930.2014.941551
19. Kang S, Jung J, Choe JK, Ok YS, Choi Y (2018) Effect of biochar particle size on hydrophobic organic compound sorption kinetics: Applicability of using representative size. Sci Total Environ 619:410–418. 10.1016/j.scitotenv.2017.11.129
20. Kim Y, Lee Y, Kim M, Park H (2019) Preparation of high porosity bricks by utilizing red mud and mine tailing. J Clean Prod 207:490–497. https://doi.org/10.1016/j.jclepro.2018.10.044
21. Lindsay M, Moncur M, Bain J, Jambor J, Ptacek C, Blowes D (2015) Geochemical and mineralogical aspects of sulfide mine tailings. Appl Geochem 57:157–177. https://doi.org/10.1016/j.apgeochem.2015.01.009
22. Liu Q, Chen B, Haderlein S, Gopalakrishnan G, Zhou Y (2018) Characteristics and environmental response of secondary minerals in AMD from Dabaoshan Mine, South China. Ecotox Environ Safe 155:50–58. https://doi.org/10.1016/j.ecoenv.2018.02.017
23. Liu S, Yang X, Chen L, Li Y, Zheng K, Hong Y (2020) Geological and geochemical characteristics and genesis of the Cishan gold deposit in Tongling ore cluster area, Anhui Province. Solid Earth Sciences 5(3):182–201. https://doi.org/10.1016/j.sesci.2020.06.003
24. Moncur MC, Ptacek CJ, Blowes DW, Jambor JL (2005) Release, transport and attenuation of metals from an old tailings impoundment. Appl Geochem 20:639–659. https://doi.org/10.1016/j.apgeochem.2004.09.019
25. Majzlan J, Plášil J, Škoda R, Gescher J, Kögler F, Rusznyak A, Küsel K, Neu T, Mangold S, Rothe J (2014) Arsenic-rich acid mine water with extreme arsenic concentration: mineralogy, geochemistry, microbiology, and environmental implications. Environ Sci Technol 48:13685–13693. https://doi.org/10.1021/es5024916

26. Martínez-Pagána P, Faz A, Acosta J, Carmona D, Martínez-Martínez S (2011) A multidisciplinary study for mining landscape reclamation: A study case on two tailing ponds in the Region of Murcia (SE Spain). Phys Chem Earth 36(16):1331–1344. https://doi.org/10.1016/j.pce.2011.02.007
27. Nikonow W, Rammlmair D, Furche M (2019) A multidisciplinary approach considering geochemical reorganization and internal structure of tailings impoundments for metal exploration. Appl Geochem 104:51–59. https://doi.org/10.1016/j.apgeochem.2019.03.014
28. Nordstrom DK (2011) Hydrogeochemical processes governing the origin, transport and fate of major and trace elements from mine wastes and mineralized rock to surface waters. Appl Geochem 26(11):1777–1791. https://doi.org/10.1016/j.apgeochem.2011.06.002
29. Orlando M, Galvão E, Cavichini A, Rangel C, Orlando C (2020) Tracing iron ore tailings in the marine environment: An investigation of the Fundão dam failure. Chemosphere 257:127184. https://doi.org/10.1016/j.chemosphere.2020.127184
30. Redwan M, Rammlmair D, Meima JA (2012) Application of mineral liberation analysis in studying micro-sedimentological structures within sulfide mine tailings and their effect on hardpan formation. Sci Total Environ 414:480–493. https://doi.org/10.1016/j.scitotenv.2011.10.038
31. Regelink I, Voegelin A, Weng L, Koopmans G, Comans R (2014) Characterization of Colloidal Fe from Soils Using Field-Flow Fractionation and Fe K-Edge X-ray Absorption Spectroscopy. Environ Sci Technol 48(8):4307–4316. https://doi.org/10.1021/es405330x
32. Rodríguez L, Ruiz E, Alonso-Azcárate J, Rincón J (2009) Heavy metal distribution and chemical speciation in tailings and soils around a Pb-Zn mine in Spain. J environ Manage 90(2):1106–1116. 10.1016/j.jenvman.2008.04.007
33. Shen ZJ, Xu DC, Li LL, Wang JJ, Shi XM (2019) Ecological and health risks of heavy metal on farmland soils of mining areas around Tongling City, Anhui, China. Environ Sci Pollut R 26(15):15698–15709. 10.1007/s11356-019-04463-0
34. Silveira LL, Sucharski GB, Pukasiewicz AGM, Paredes RSC (2018) Influence of particle size distribution on the morphology and cavitation resistance of high-velocity oxygen fuel coatings. J Therm Spray Techn 27(4):695–709. 10.1007/s11666-018-0708-0
35. Singh KP, Mohan D, Singh VK (2005) Studies on distribution and fractionation of heavy metal in Gomti river sediments-a tributary of the Ganges, India. J Hydrol 312(1–4):14–27. https://doi.org/10.1016/j.jhydrol.2005.01.021
36. Tuhý M, Hrstka T, Ettler V (2020) Automated mineralogy for quantification and partitioning of metal(loid)s in particulates from mining/smelting-polluted soils. Environ Pollut 266(1):115118. https://doi.org/10.1016/j.envpol.2020.115118
37. Tang J, Zhou C, Wang X, Xiao X, Lü Q (2013) Deep electrical structure and geological significance of Tongling ore district. Tectonophysics 606:78–96. https://doi.org/10.1016/j.tecto.2013.05.039
38. Theoharatos C, Ifantis A, Laskaris NA, Economou G (2008) Charting of geoelectric potential signal dynamics via geometrical techniques and its possible relation to significant earthquakes in Western Greece. Comput Geosci-UK 34(6):625–634. https://doi.org/10.1016/j.cageo.2007.06.006

39. Tang Q, Sheng W, Li L, Zheng L, Miao C, Sun R (2018) Alteration behavior of mineral structure and hazardous elements during combustion of coal from a power plant at Huainan, Anhui, China. Environ Pollut 239:768–776. https://doi.org/10.1016/j.envpol.2018.04.115
40. Xu DC, Zhou P, Zhan J, Gao Y, Dou CM, Sun QY (2013) Assessment of trace metal bioavailability in garden soils and health risks via consumption of vegetables in the vicinity of Tongling mining area, China. Ecotox Environ Safe 90:103–111. https://doi.org/10.1016/j.ecoenv.2012.12.018
41. Yang Y, Li Y, Sun Q (2014) Archaeal and bacterial communities in acid mine drainage from metal-rich abandoned tailing ponds. Tongling China T Nonferr Metal Soc 24(10):3332–3342. https://doi.org/10.1016/S1003-6326(14)63474-9
42. Zarroca M, Linares R, Velásquez-López P, Roqué C, Rodríguez R (2015) Application of electrical resistivity imaging (ERI) to a tailings dam project for artisanal and small-scale gold mining in Zaruma-Portovelo, Ecuador. J Appl Geophys 113:103–113. https://doi.org/10.1016/j.jappgeo.2014.11.022
43. Zanuzzi A, Arocena JM, Van Mourik JM, Cano AF (2009) Amendments with organic and industrial wastes stimulate soil formation in mine tailings as revealed by micromorphology. Geoderma 154(1–2):69–75. https://doi.org/10.1016/j.geoderma.2009.09.014
44. Zheng LG, Chen X, Dong X, Wei X, Jiang C, Tang Q (2019a) Using δ34S–SO4 and δ18O–SO4 to trace the sources of sulfate in different types of surface water from the Linhuan coal-mining subsidence area of Huaibei, China. Ecotox Environ Safe 181:231–240. https://doi.org/10.1016/j.ecoenv.2019.06.001
45. Zhang LQ, Zhou HH, Chen X, Liu GJ, Jiang CL, Zheng LG (2021) Study of the micromorphology and health risks of arsenic in copper smelting slag tailings for safe resource utilization. Ecotox Environ Safe 219:112321. https://doi.org/10.1016/j.ecoenv.2021.112321
46. Zheng LG, Qiu Z, Tang Q, Li Y (2019b) Micromorphology and environmental behavior of oxide deposit layers in sulfide-rich tailings in Tongling, Anhui Province, China. Environ Pollut 251:484–492. https://doi.org/10.1016/j.envpol.2019.04.131
47. Zhang ZQ, Wang GW, Ding YN, Carranza EJM (2020) 3D mineral exploration targeting with multi-dimensional geoscience datasets, Tongling Cu(-Au) District, China. J Geochem Explor 221:106702. https://doi.org/10.1016/j.gexplo.2020.106702
48. Zhou HH, Liu GJ, Zhang LQ, Zhou CC (2021) Mineralogical and morphological factors affecting the separation of copper and arsenic in flash copper smelting slag flotation beneficiation process. J Hazard Mater 401:123293. https://doi.org/10.1016/j.jhazmat.2020.123293
49. Zhang W, Long JH, Wei ZY, Alakangas L (2016) Vertical distribution and historical loss estimation of heavy metals in an abandoned tailings pond at HTM copper mine, northeastern China. Environ Earth Sci 75(22):1462. 10.1007/s12665-016-6271-4

Figures

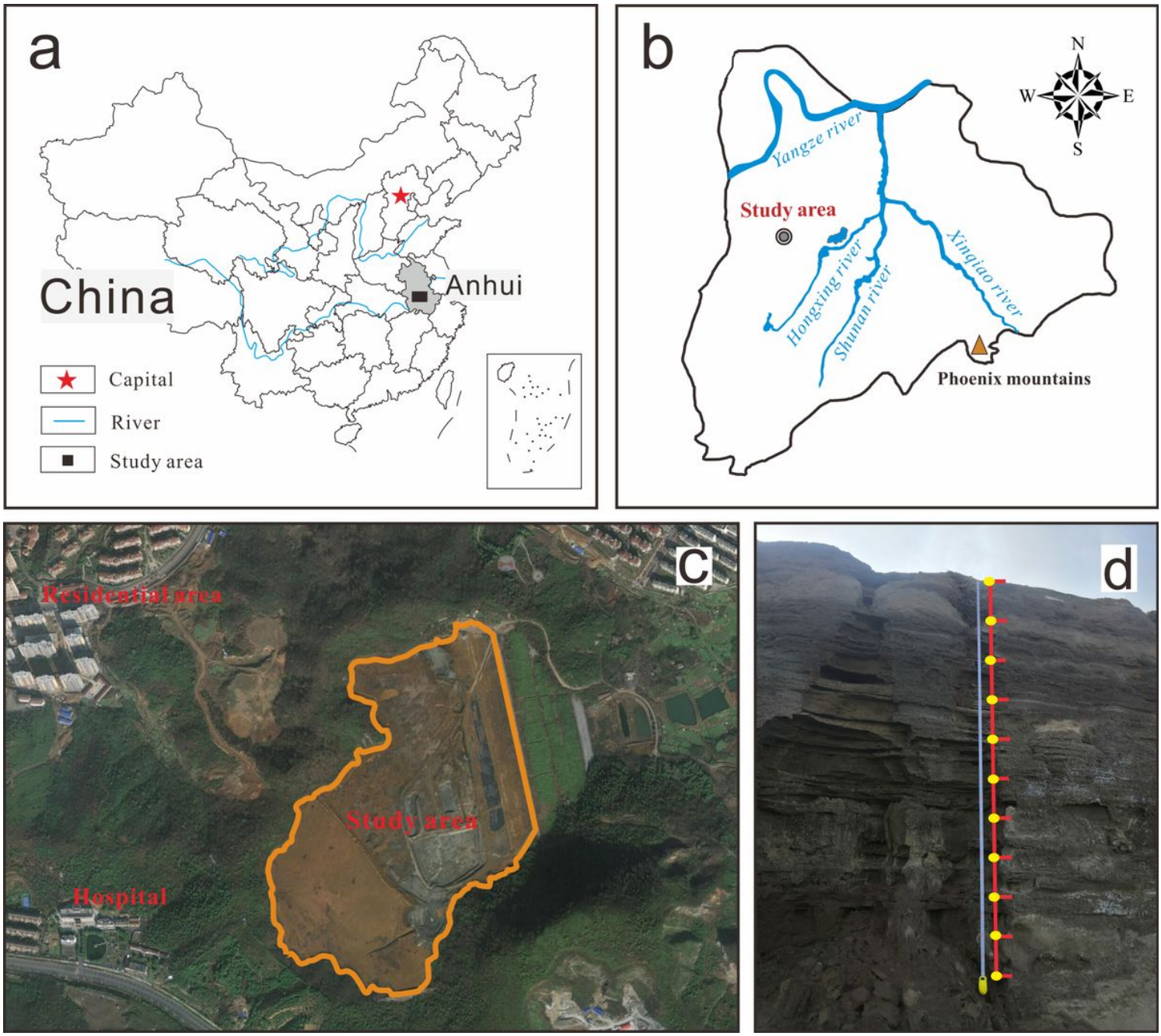

Figure 1

Geographic satellite and sampling site map of the study area Note: The designations employed and the presentation of the material on this map do not imply the expression of any opinion whatsoever on the part of Research Square concerning the legal status of any country, territory, city or area or of its authorities, or concerning the delimitation of its frontiers or boundaries. This map has been provided by the authors.

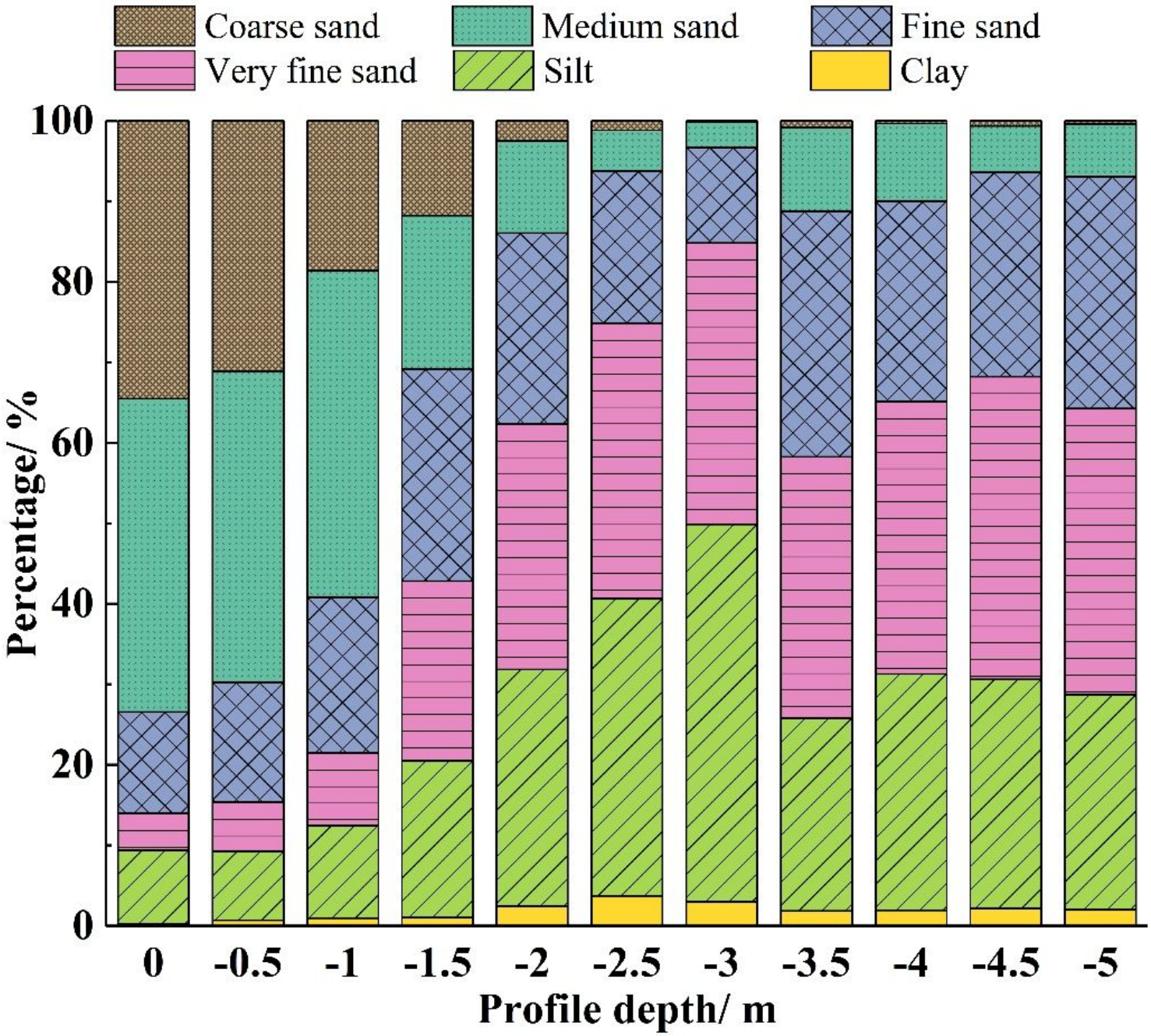

Figure 2

Particle-size distribution of tailings profile

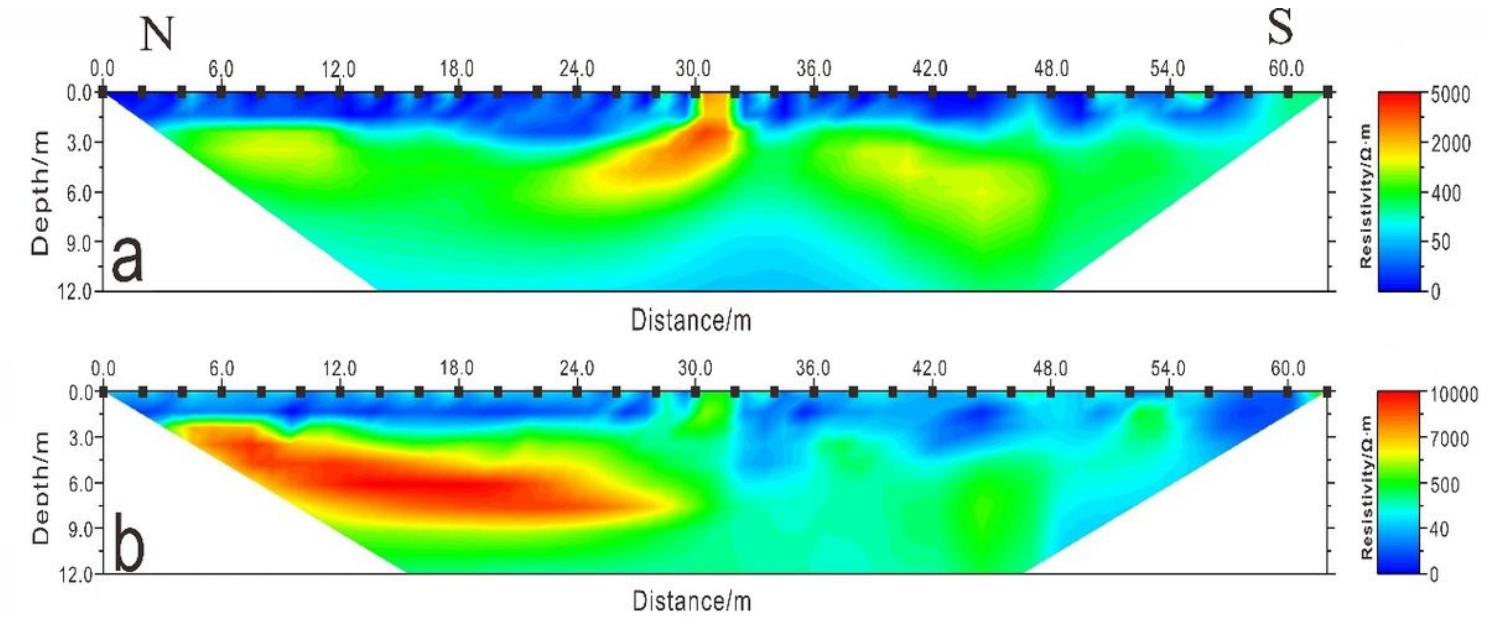

Figure 3

Apparent resistivity of tailings profile

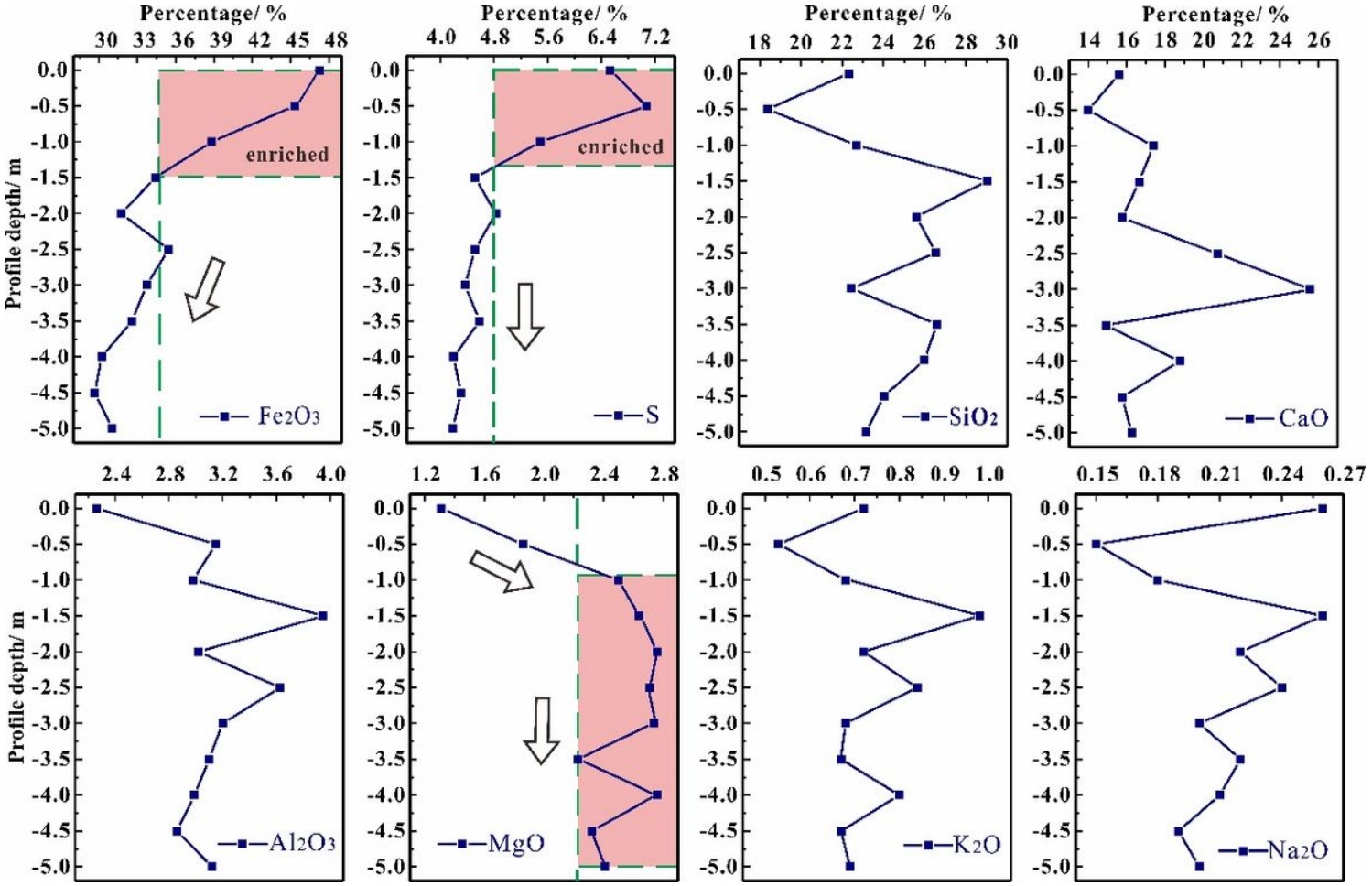

Figure 4

Major element distribution of tailings profile

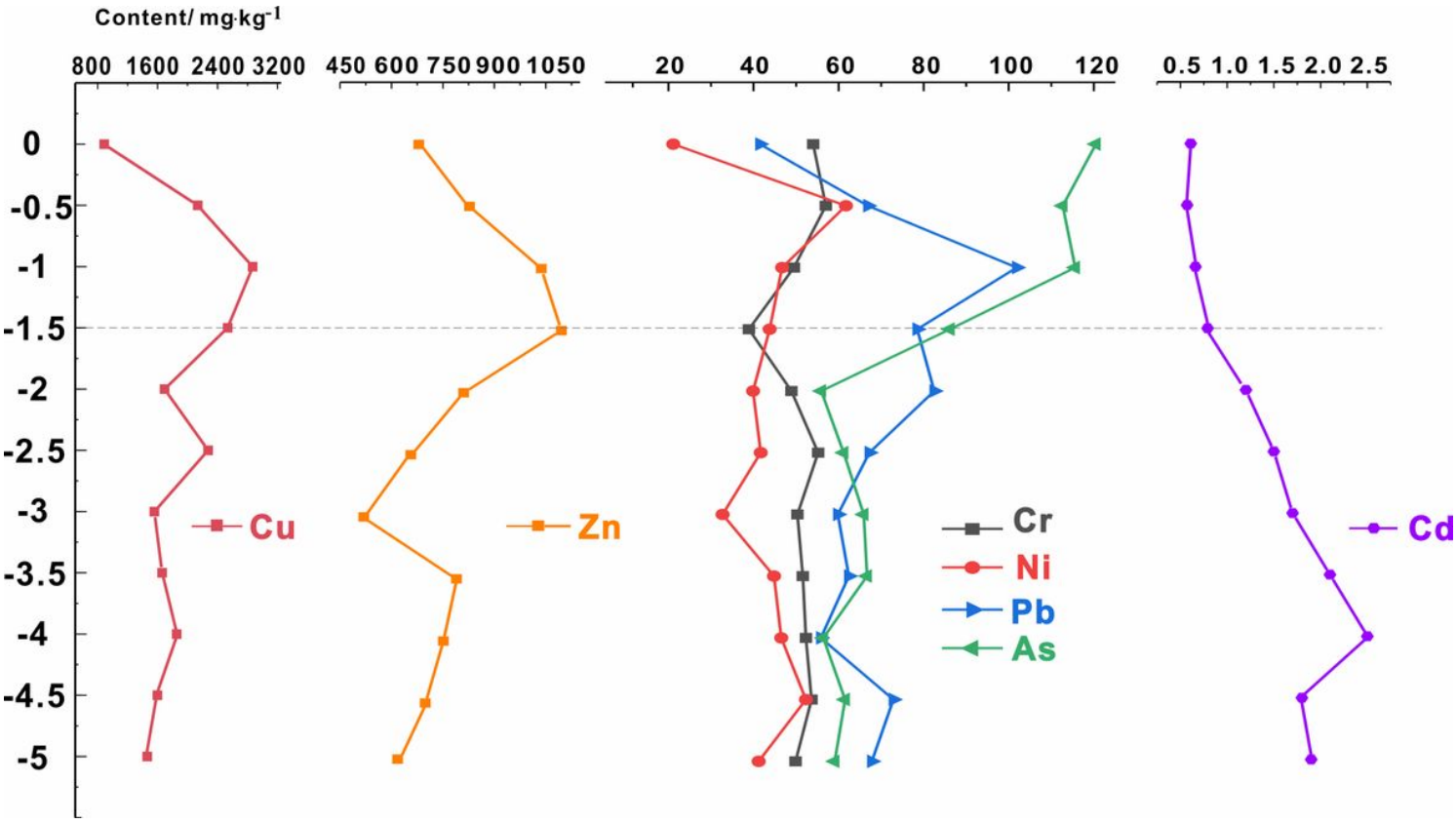

Figure 5

Heavy metal distribution of tailings profile

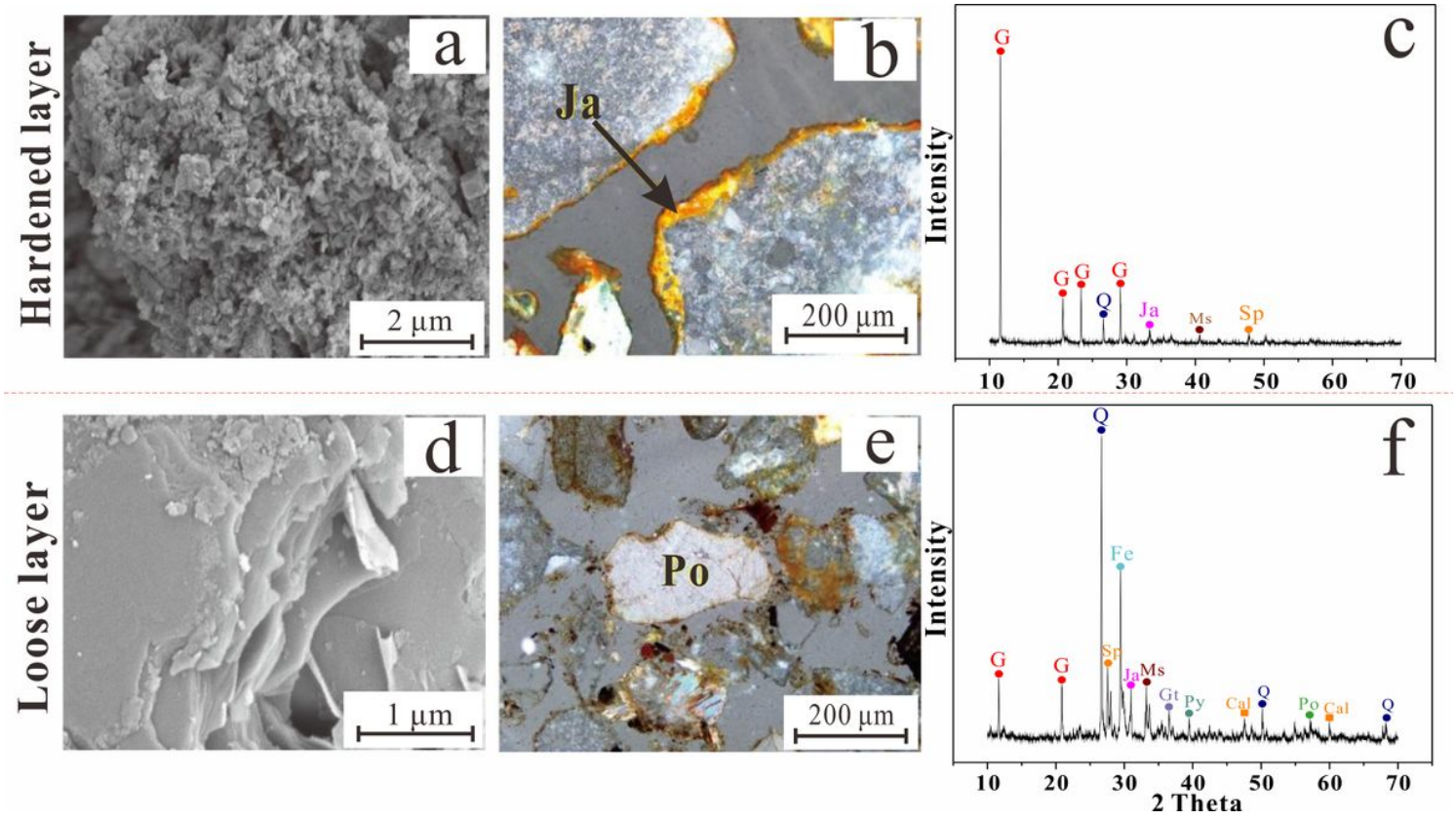

Figure 6

Mineralogy of tailings profile (a, d-SEM; b, e-Polarized light microscopy; c, f-XRD); (G-Gypsum; Q-Quartz; Ja-Jarosite; Ms-muscovite; Sp-Sphalerite; Fe- Feldspar; Gt-Goethite; Py-Pyrite; Cal-Calcite; Po-Pyrrhotite)

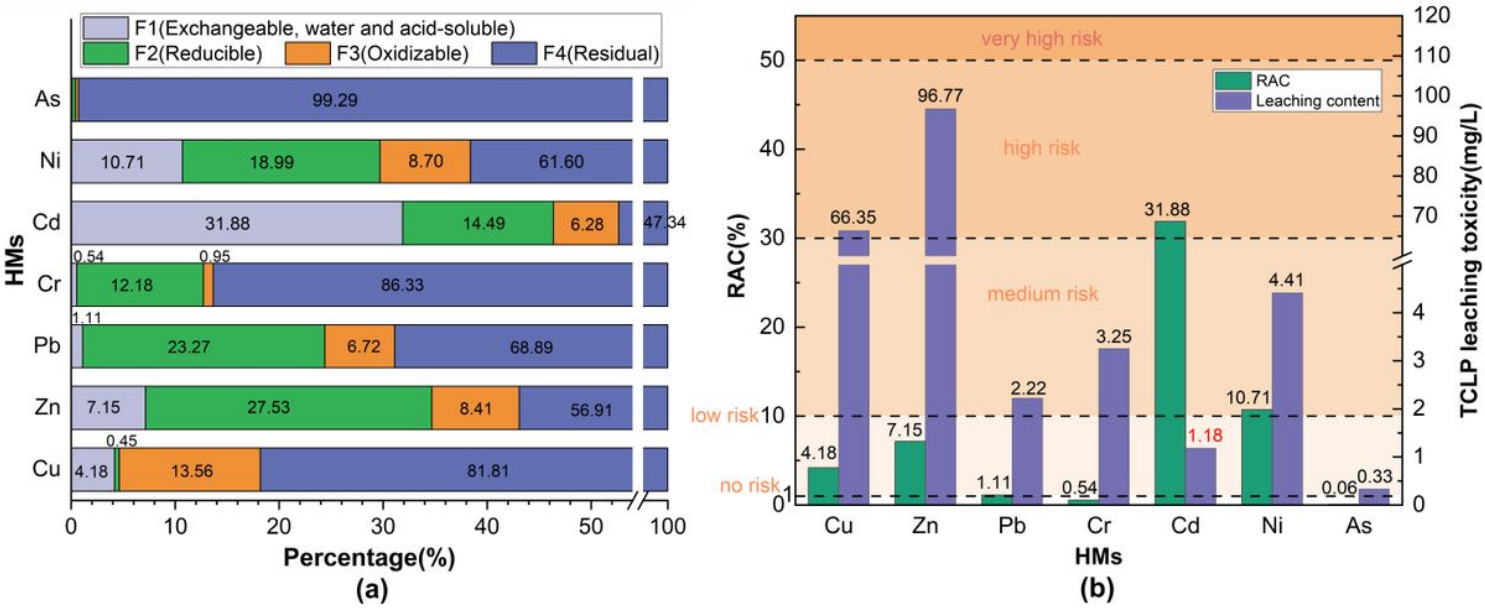

Figure 7

Chemical fraction distribution (a), leaching toxicity and risk assessment (b) of HMs in representative composite tailing sample. The filled areas of different colors represent different risks of RAC, and the red data in TCLP represents that the leaching content of HMs exceeds its standard value.

Supplementary Files

This is a list of supplementary files associated with this preprint. Click to download.

- SupplementaryMaterial.docx